EUROPEAN ORGANIZATION FOR NUCLEAR RESEARCH

CERN/EP 79-137
8 November 1979

RESULTS OF THE CERN NA3 EXPERIMENT ON MUON PAIR PRODUCTION IN HADRON COLLISIONS

CEN Saclay[1]-CERN[2]-Collège de France[3]-E.P. Palaiseau[4]-
LAL Orsay[5] Collaboration

J. Badier[4], J. Boucrot[5], G. Burgun[1], O. Callot[5], P. Charpentier[1],
M. Crozon[3], D. Decamp[2], P. Delpierre[3], A. Diop[3], R. Dubé[5],
B. Gandois[1], R. Hagelberg[2], M. Hansroul[2], W. Kienzle[2],
A. Lafontaine[1], P. Le Dû[1], J. Lefrançois[5], T. Leray[3], G. Matthiae[2],
A. Michelini[2], P. Miné[4], H. Nguyen Ngoc[5], O. Runolfsson[2],
P. Siegrist[1], J. Timmermans[2], R. Vanderhaghen[4], J. Valentin[3]
and S. Weisz[2]

presented by W. Kienzle

The present report reviews the results of the CERN NA3 Experiment on muon pair production by tagged hadron beams ($\pi^{\pm}$, $K^{\pm}$, $\bar{p}$ and p) at 200 (280) GeV/c.

The original aim of the experiment proposed in summer 1974 was "the study of lepton-hadron correlations at large p_t". As a running-in experiment we have measured the inclusive production of muon pairs in order to obtain the structure functions of unstable particles (π, K) by making use of the Drell-Yan process. Furthermore as a by-product we have obtained the J/ψ and the upsilon (Υ) resonances, the Υ being observed with a pion beam for the first time.

Presented at the International Symposium on
Lepton and Photon Interactions at High Energies
Fermilab, August 1979

WK/ed

The following subjects will be discussed:

1. The experimental equipment
   - 1.1 Tagged hadron beam
   - 1.2 Targets and beam dump
   - 1.3 The spectrometer system
   - 1.4 Triggering system
   - 1.5 Acceptance
   - 1.6 Data taking and analysis
2. Results
   - 2.1 Production of Υ resonance(s) by pions
   - 2.2 High-mass continuum and the Drell-Yan model
   - 2.3 Structure function of the pion
3. Summary and conclusions

For details we refer to our publications [1-4].

1. THE EXPERIMENTAL EQUIPMENT

The apparatus is shown schematically in fig. 1(a) and photographed in fig. 1(b); this is basically a beam dump experiment using a tagged hadron beam and a large acceptance magnetic spectrometer for dimuon detection.

1.1 Tagged hadron beam

We have been using an unseparated secondary hadron beam produced by 400 GeV protons on a 50 cm Be target. Particle identification is done by two differential Cerenkov counters (CEDAR) for $K^{\pm}$ and $\bar{p}$, and by two threshold Cerenkov counters for π^{+}. Beam intensities used in the experiment are in the range from 1-5 $\times$ 10^{7} particles/pulse. At 200 GeV/c the fraction of π^{+} and K^{+} in the positive beam after filtering by a 2 m long CH_2 absorber, was 36% and 4.6%, respectively. Details are shown in table 1.

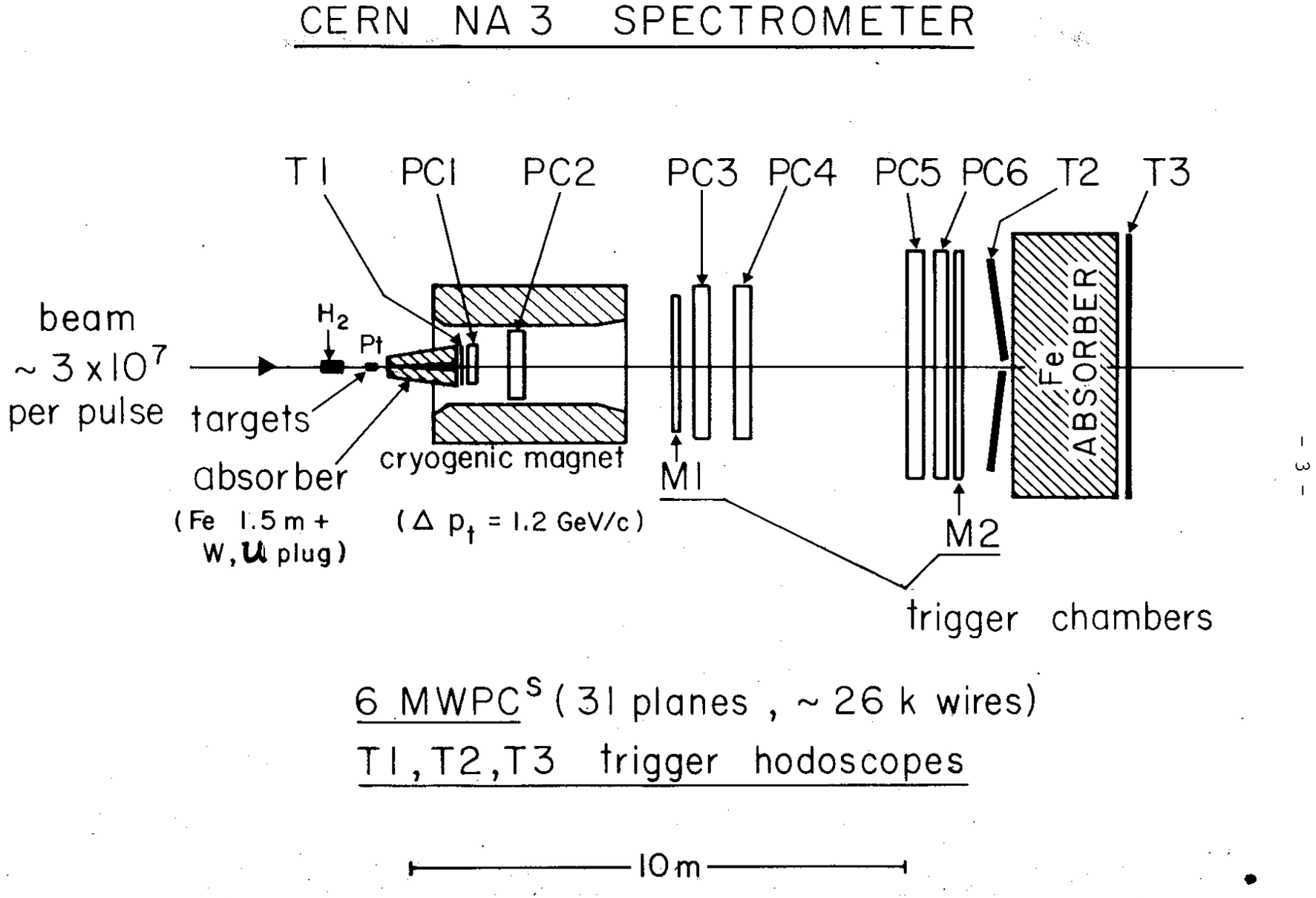

Fig. 1 (a) Layout of the NA3 spectrometer (schematically)

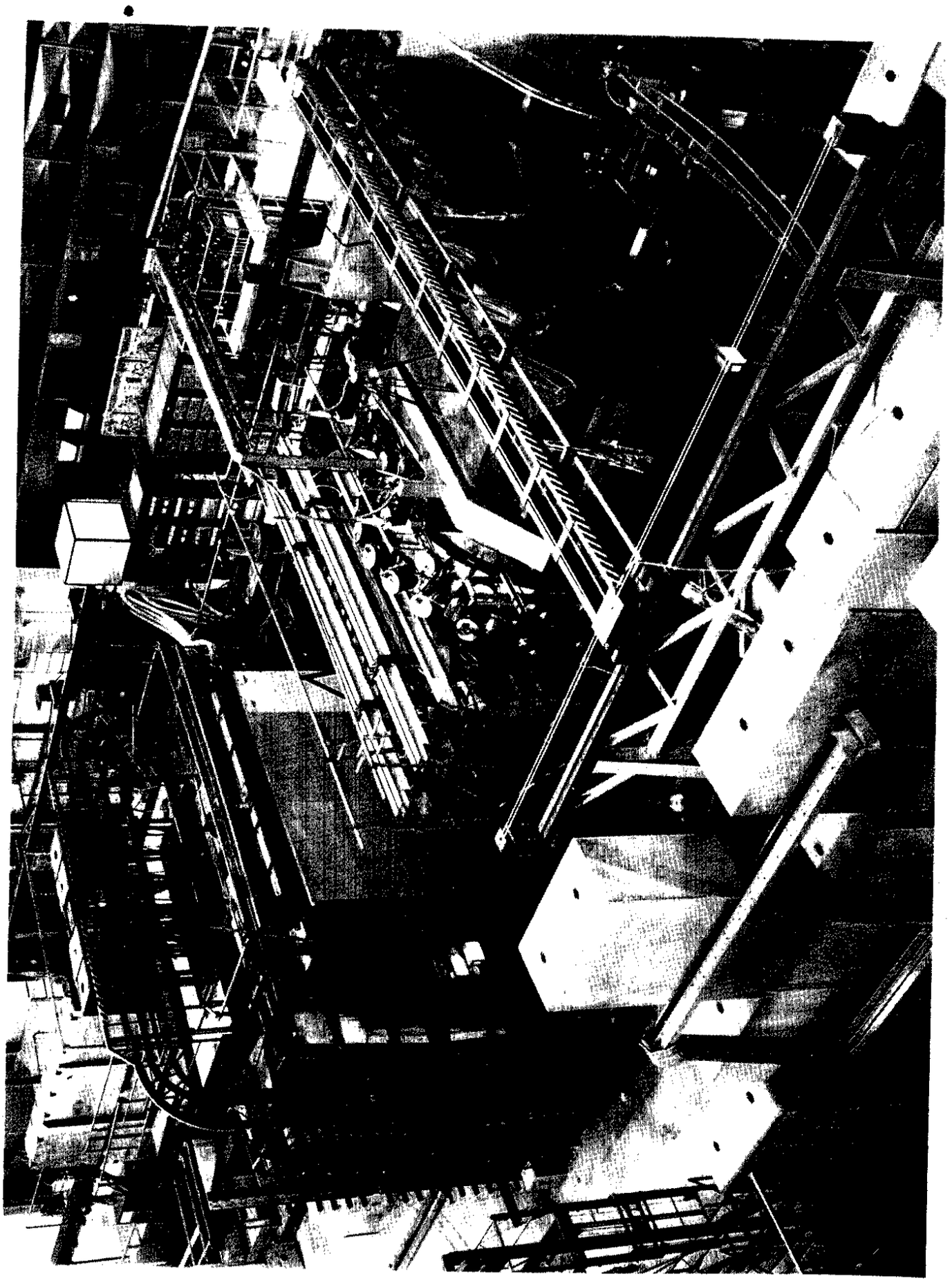

Fig. 1(b)

TABLE 1

CERN SPS 400 GeV protons ($1-3 \times 10^{12}$ ppp) → 50 cm Be → H8 beam North Area. Beam composition:

⊖ beam

Particle	π^-	K^-	$\bar{p}$
Ratio per cent	96.3	3.1(*)	0.6(*)
Identification	-	CD1	CD2

2 differentail CD^S = "CEDARS" : 8 PM^S → 8 TDC^S

⊕ beam

Particle	π^+	K^+	p
Ratio per cent	36.0	4.6	59.4
Identification	C1-C2	CD1-CD2	-

2m Ch_2 absorber (π^+/p)

2 differential CD^S

2 threshold $C^S(\pi^+)$

The time resolution of the tagging system of $\sigma(t) \approx 0.6$ ns determines the maximum acceptable particle flux due to random background which we limit to $\sim$ 20% for $\bar{p}$ and K^-.

1.2 Targets and beam dump

A novel feature of this experiment is the simultaneous use of a (30 cm) hydrogen and a heavy nuclear (platinum) target; this allows interesting studies of the absolute per (free) nucleon cross section as well as the A-dependence of the Drell-Yan (DY) process. Platinum

(*) Note that at -150 GeV/c we have now 4.5% and 2% K^- and $\bar{p}$ fractions, respectively; the increase in relative $\bar{p}$ flux has been achieved after optimization of the target length and production angle.

targets, 6 cm in length for the 200 GeV/c runs and 11 cm for the 280 GeV/c runs were used. They were placed 40 cm upstream of a dump consisting of a 1.5 m long block of stainless steel with a heavy (tungsten-uranium) conical plug of ±30 mrad aperture inserted in the centre. The diameter of the Pt target (12 mm) and the tip of the dump (20 mm) were matched to a beam size of σ = 3-4 mm. The target configuration and their separation by reconstructed events are illustrated in fig. 2.

1.3 The spectrometer system (fig. 1)

This has been designed for high acceptance in order to be able to study dileptons in a wide range of kinematic variables. It consists of:

(a) a large superconducting dipole magnet with a vertical field ($\int$Bdl ~ 4.0 Tm) in a cylindrically shaped air gap of 1.6 m diameter;

(b) a set of six multiwire proportional chambers (31 planes with a total of $\sim$ 26 000 wires) ranging in size from 0.6 × 0.6 m^2 to 4.2 × 4.0 m^2;

(c) a muon filter composed of 12 cm of lead and 1.8 m of iron, placed in front of the last triggering hodoscope T3.

The spectrometer is composed of two symmetric telescopes of counters and chambers placed above and below the beam axis. They are covering vertical laboratory angles between ±6 and ±165 mrad. For the mass resolution we refer to fig. 3, below; a typical value is $\sigma \approx 4\%$ and slightly mass dependent.

1.4 Triggering system

A two-level trigger was used to minimize the electronics dead time due to the high particle flux in the chambers. The trigger elements are shown in fig. 4. A "pretrigger" is provided by three planes of counter hodoscopes:

(a) T1 placed at the end face of the beam dump consisting of 12 counters.

(b) T2 which is subdivided into 42 horizontal strips.

(c) T3 situated behind the iron wall, made of 22 horizontal strips.

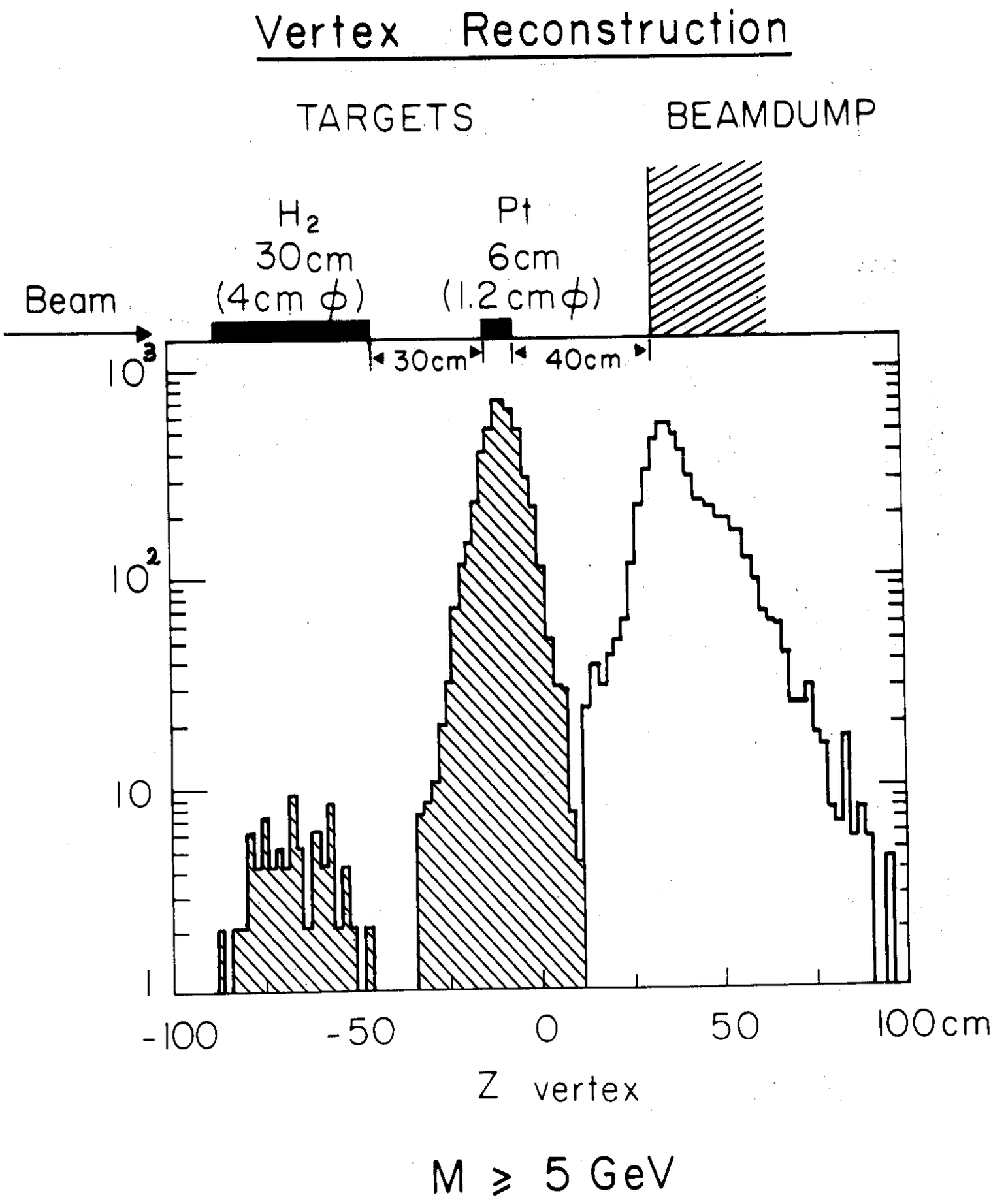

Fig. 2 Vertex reconstruction : separation of the targets from the beam dump.

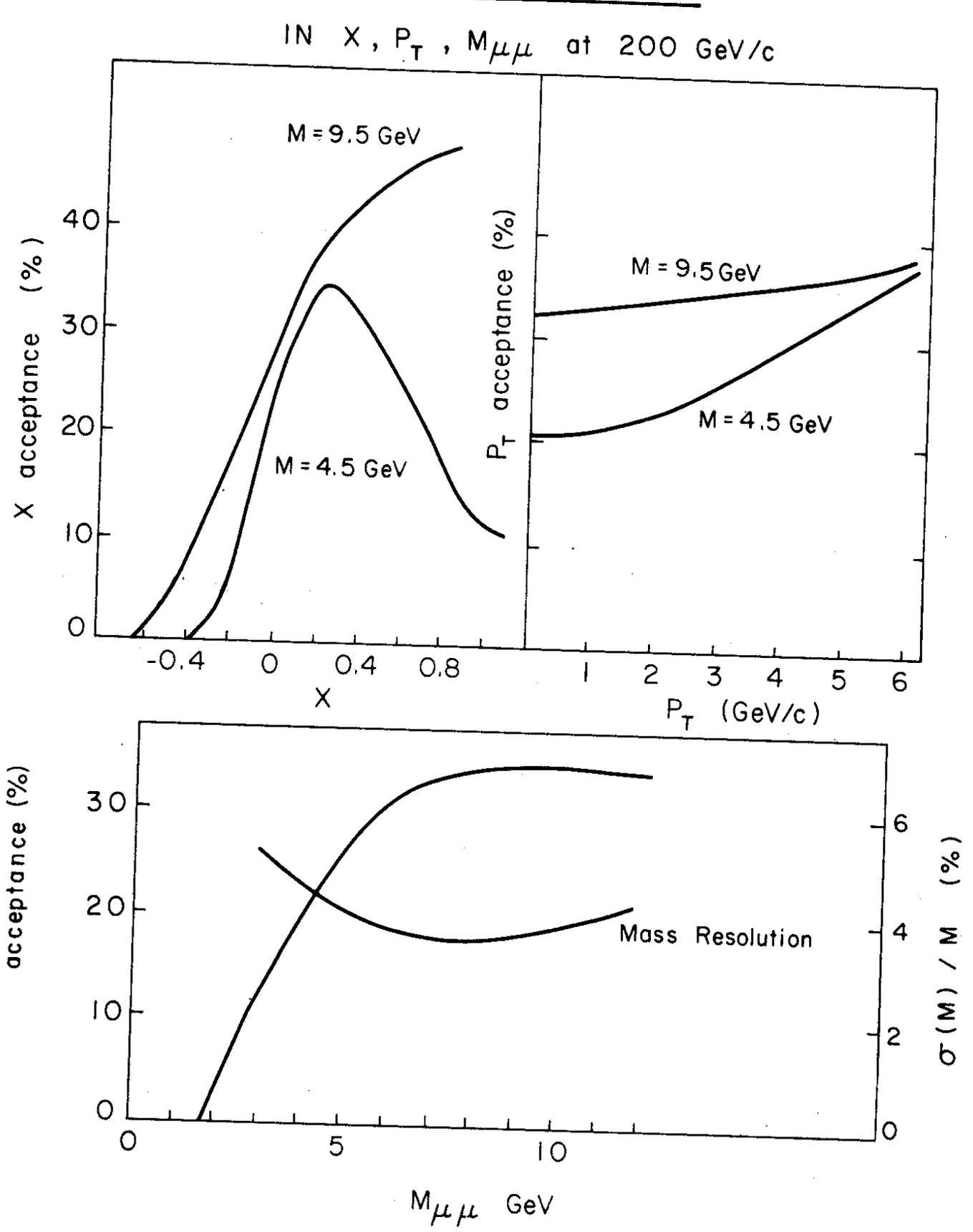

Fig. 3 Acceptance vs. x, Pt and M of the di-muons.

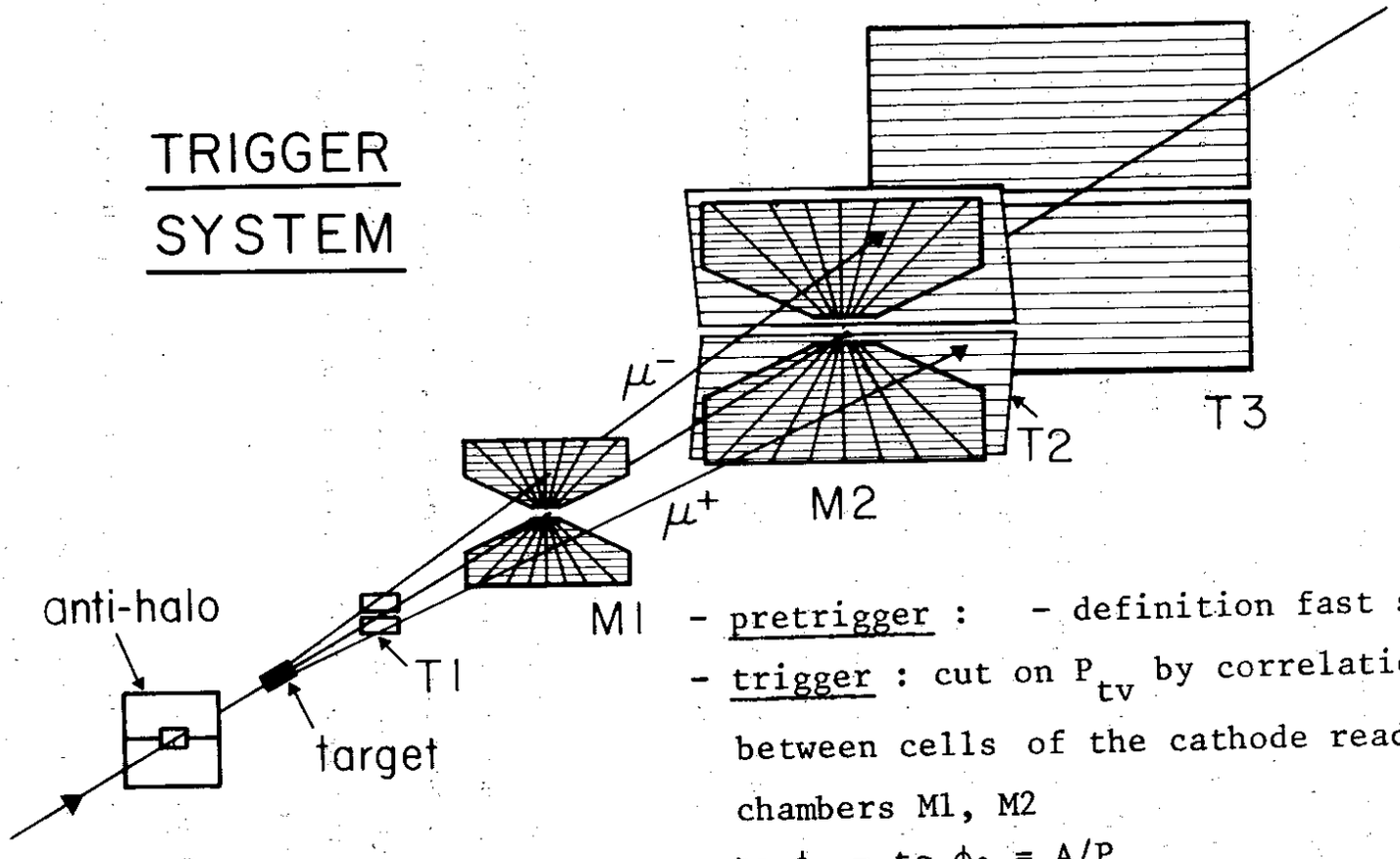

- pretrigger : - definition fast strobe
- trigger : cut on P_{tv} by correlations between cells of the cathode read-out chambers M1, M2

$$\text{tg } \phi_1 - \text{tg } \phi_2 = A/P_{tv}$$

rough cut on $M_{\mu\mu} > 2$ GeV

- one muon : $P_{tv} > 1$ GeV/c
- both muons : $P_{tv} > 0.7$ GeV/c

Fig. 4 Trigger system.

The "pretrigger" which requires at least two particles in the coincidence T2, T3 and at least one particle in T1, provides a fast strobe for the proportional chambers PC1, PC2, M1 and M2. The pretrigger signal is vetoed by an $\sim$ 1 m^2 halo counter placed upstream of the target. The "trigger" proper acts on the vertical component p_t^v of the transverse momentum of the muons. The p_t^v selection is achieved by two planes of cathode read-out chambers M1 and M2, covering vertical angles from ±30 mrad up to ±165 mrad and an overall azimuthal acceptance of 2/3. The cathodes are printed in 18 separate horizontal bands, each subdivided into 64 cells corresponding to equal intervals of the tangent of the azimuthal angle. The correlation between cells of a given band provides a cut-off in the magnetic deflection angle and thus in p_t^v, which in turn, defines a rough lower cut on the muon pair effective mass. The trigger conditions in the course of the experiment were either $p_t^v > 0.7$ GeV/c for both muons, or $p_t^v > 1$ GeV/c for one muon, without a cut on the other muon.

1.5 Acceptance

The overall acceptance of the apparatus at 200 GeV/c, as determined by the geometry of the detectors and by the p_t^v cut, is shown in fig. 3 as a function of the dimuon fractional momentum x, the transverse momentum p_t, and the dimuon mass (also shown is the dimuon mass resolution). Note that the acceptance value at high masses is better than 30% and almost mass-independent.

1.6 Data taking and analysis

A typical rate of data acquisition is of the order of 30 triggers/pulse or $\sim$ 2-3 × 10^5 events per day written on magnetic tape, or 3-5 × 10^6 events per run. The quality of the trigger is illustrated by the percentage of dimuons which is typically 50-60%, with 2-3 J/ψ^s per pulse or 20 000 J/ψ^s per day; the J/ψ events serve as a very useful calibration signal in the off-line analysis.

Pattern recognition of both muons is performed in the spectrometer chambers with an overall efficiency of (94 ± 2)%, measured from visual scanning of a sample of reconstructed events. The off-line processing time per event is 20-30 ms. The data reported here represent a total of about 10^7 triggers.

2. RESULTS

The data reported have been taken between September 1978 and May 1979, with negative and positive beams of 200 (280) GeV/c, the number of events for the different channels are summarized in table 2.

The sensitivity of the experiment is demonstrated by the sample of altogether more than 15 000 DY events, and the presence of > 500 000 J/ψ^s as a byproduct. The amount of π-induced DY data is substantially beyond earlier experiments, especially for π^+; the H_2 data are unique but still scarce; the same is true for the highly interesting K^- and $\bar{p}$ events which we hope, however, to increase by an order of magnitude by the end of the year.

TABLE 2

Data (September 1978 - May 1979)

	Pt target		H_2 target	
	J/ψ	M > 4 GeV	J/ψ	M > 4 GeV
π^- 280 GeV/c	130 000	5700	-	-
⊖ 200 GeV/c	145 000	5916	3000	138
K^-	2 800	119	56	1
$\bar{p}$	1 000	44	17	0
⊕ π^+	108 000	2195	2200	45
K^+	16 000	215	340	2
p	101 000	1304	2200	23

2.1 Production of Υ resonance(s) by pions

The overall dimuon mass distribution is shown in fig. 5; apart from a very abundant J/ψ peak(*) at the low mass end, we observe here for the first time upsilon production by pions. The Υ : J/ψ cross section ratio is 2×10^{-4}. With our mass resolution of $\sigma \approx 4\%$ we are, unfortunately, unable to resolve the Υ substates.

We show here the positive beam data which are particularly well suited for resonance spectroscopy since the physical "background" is 3-4 times less than for π^- events (on nuclear targets) due to the charge asymmetry of the DY process (note that the technical background is entirely negligeable). The signal-to-background ratio of the Υ is ~ 4 with 54 ± 12 events above background (table 3(a)).

The negative beam data are shown in fig. 6 where the Υ signal appears less prominent for reasons as discussed, however with a production cross section compatible with the π^+ data.

The Υ is more easily observed with π beams since the π/p cross section ratio is as large as 30 which can be understood in the framework of a light quark fusion model of the Υ production mechanism (table 3(b)).

TABLE 3

(a) Υ production by pions

	π^+ 200 GeV/c	π^- 200 GeV/c	π^- 280 GeV/c
$N_{\Upsilon + \Upsilon' + \Upsilon''}$	53 ± 12	55 ± 15	66 ± 20
$B\sigma(\Upsilon's)$ pb/nucleon	1.9 ± 0.6	1.5 ± 0.5	2.4 ± 0.9
$\frac{B\sigma(\Upsilon's)}{B\sigma(J/\psi)}$	$(2.4 \pm 0.6)10^{-4}$	$(1.9 \pm 0.5)10^{-4}$	$(2.2 \pm 0.7)10^{-4}$

(*) A detailed study of J/ψ production by different incident particles on H_2 and Pt targets has been published elsewhere [2].

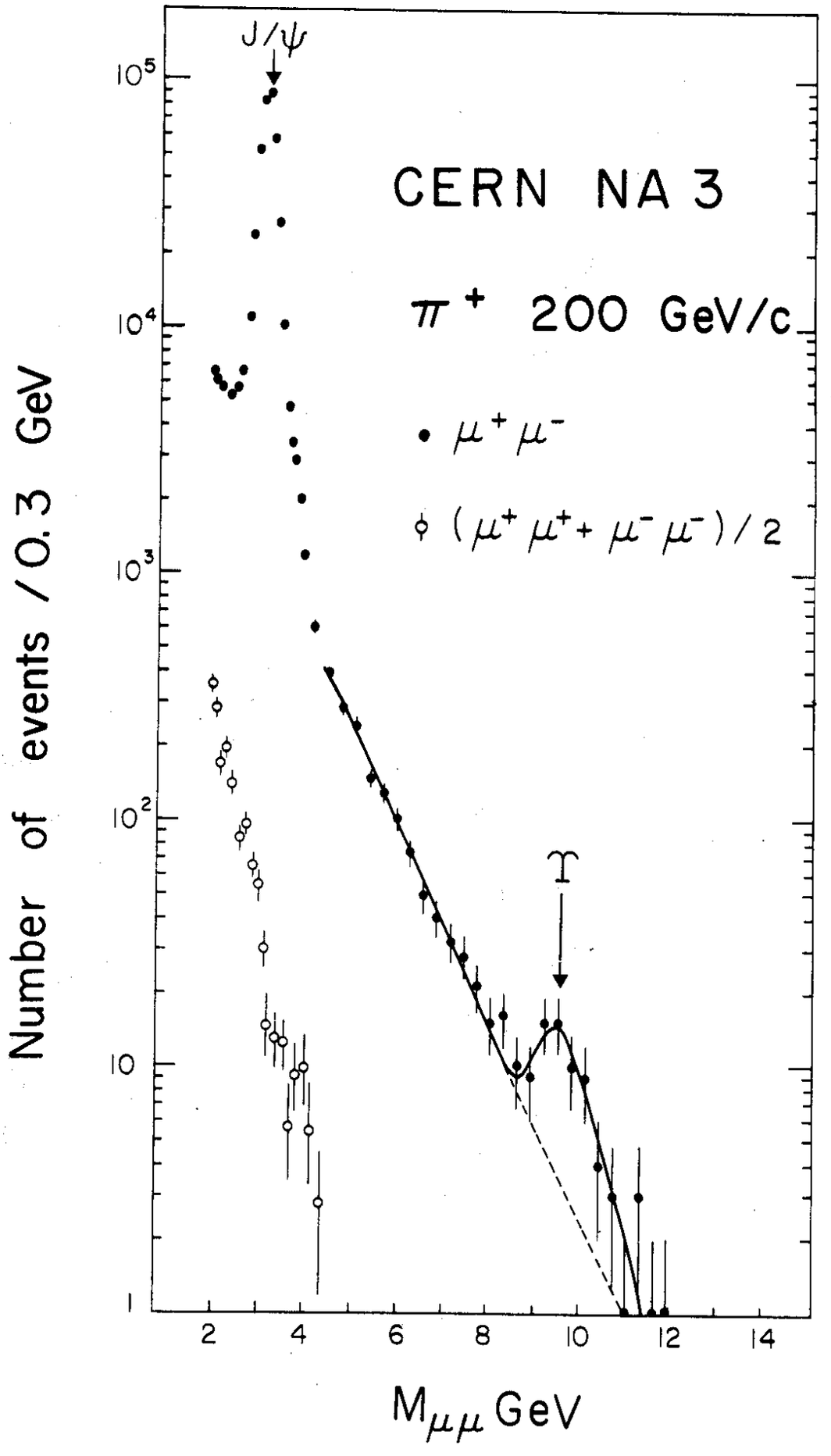

Fig. 5 Di-muon mass distribution for π^+ at 200 GeV/c.

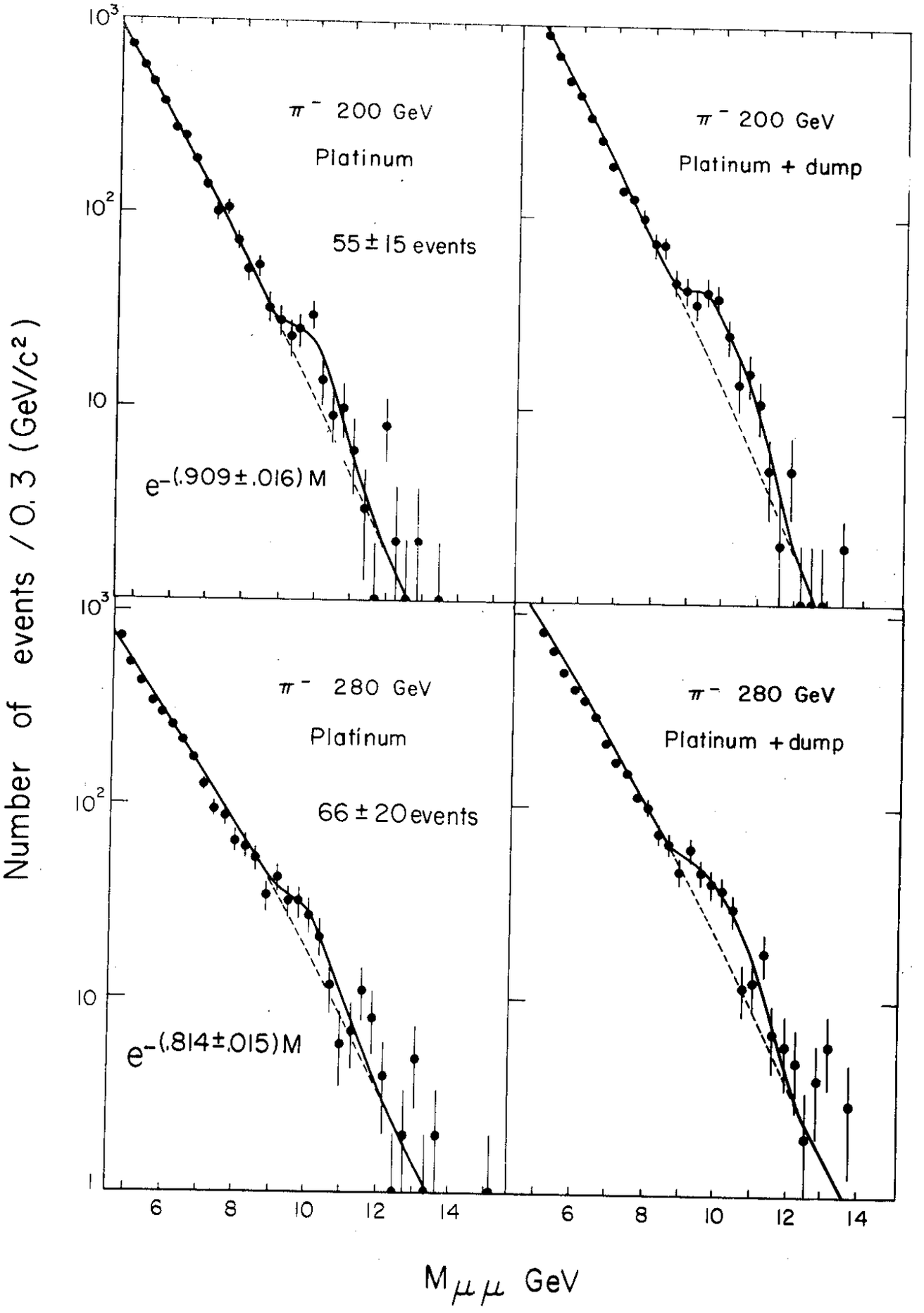

Fig. 6 Di-muon mass distribution for π^- at 200 and 280 GeV/c.

(b) Cross section ratios for Υ production

K^+/π^+	0.34 ± 0.23	0.10
p/π^+	0.03 ± 0.02	0.05
π^-/π^+	0.76 ± 0.29	0.83

light quark fusion model using NA3 structure functions

A comparison of pion and proton cross sections for Υ production as a function of $\tau = M/\sqrt{s}$ is shown in fig. 7.

The relative lack of background in the π^+ channel allows a rather clean study of the resonance such as for example the x distribution shown in fig. 8; the asymmetric x distribution with $\langle x \rangle \approx 0.2$ is a consequence of the difference between the quark structure of the pion and the nucleon.

We have also examined the Υ decay angular distribution (not shown here) and find it compatible with flat, in contrast to the adjacent DY continuum events.

The various parameters of our Υ results have been summarized in table 3.

2.2 High-mass continuum and the Drell-Yan process

The original aim of this experiment has been a measurement of the quark structure of unstable hadrons (π, K) by use of the DY process. The DY model provides a simple description of lepton-pair production in hadronic reactions where a quark and an antiquark of the beam and target particles annihilate electromagnetically into a virtual photon with subsequent decay into an e^+e^- or a $\mu^+\mu^-$ pair.

Measurement of the lepton pair's invariant mass M and fractional momentum x uniquely determine the x_1 and x_2 of the annihilating quarks in the projectile and target particle; thus their structure functions can be extracted.

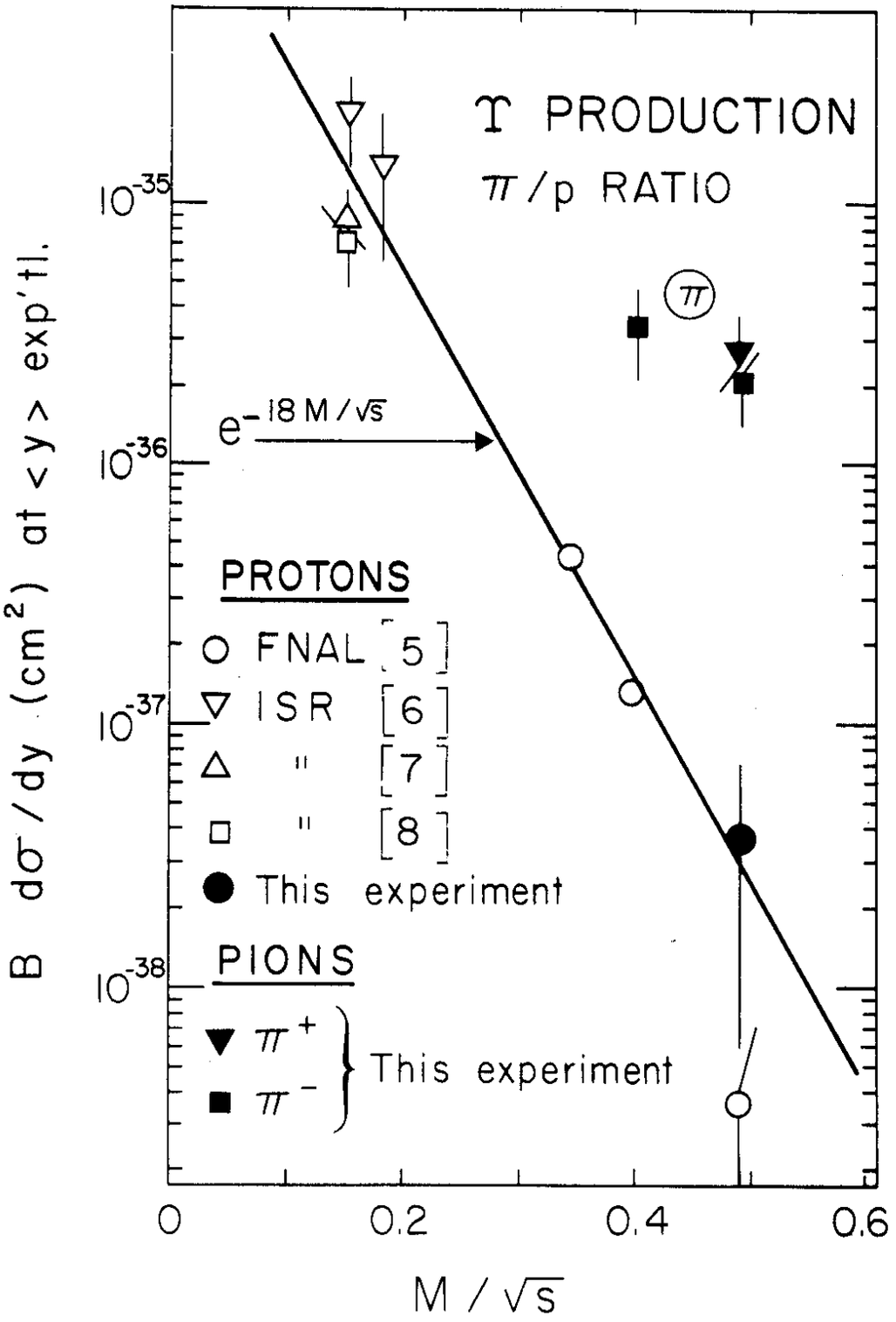

Fig. 7 Cross section comparison between protons and pions for Υ production.

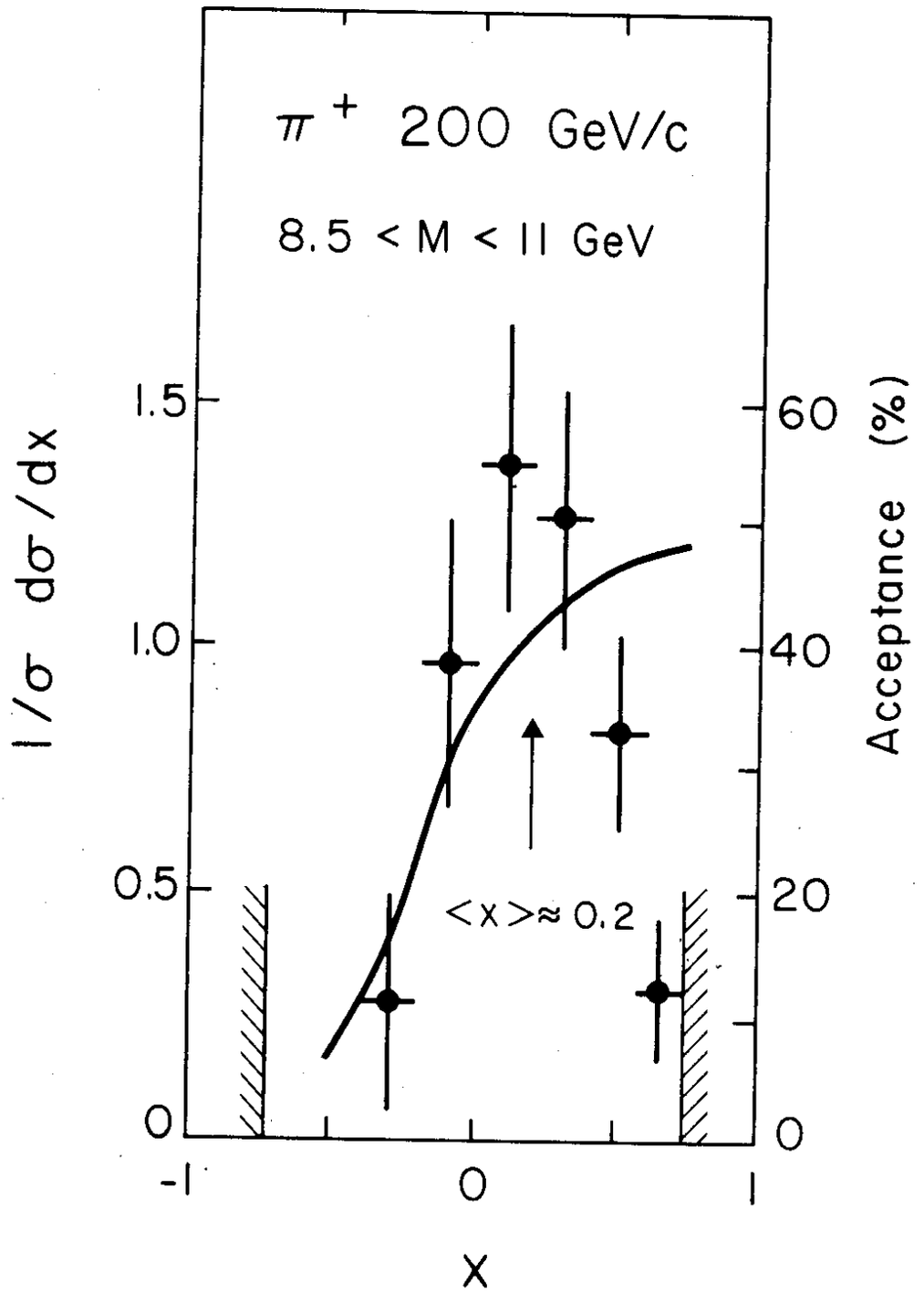

Fig. 8 X - distibution for T events.

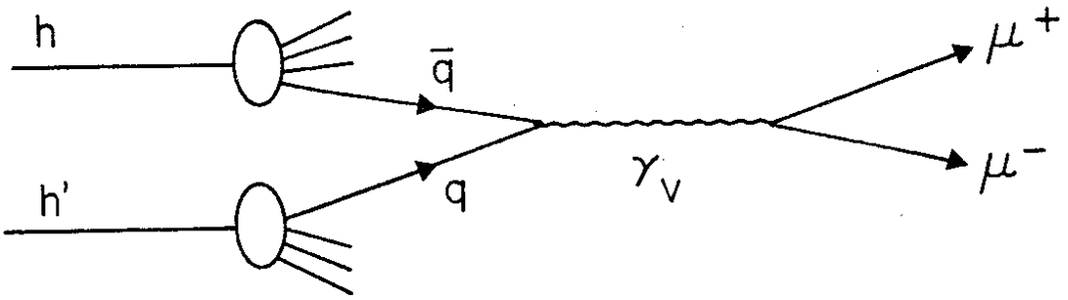

We measure

$$M_{\mu\mu}^2 = x_1 x_2 s$$

$$X_{\mu\mu} = x_1 - x_2 = \frac{2P_L^*}{\sqrt{s}} \Bigg\} \text{ calculate } x_1,\ x_2,\ d^3\sigma/dM\,dx_1dx_2 \text{ } (p_t \text{ neglected}).$$

Extract structure functions $f(x_1)$, $f(x_2)$

$$\frac{d^2\sigma}{dx_1\,dx_2} = \frac{4\pi\alpha^2}{3s}\frac{1}{3}\sum_i \frac{Q_i^2}{x_1^2 x_2^2}\left[f_i^h(x_1)\, f_{\bar{i}}^{h'}(x_2) + f_{\bar{i}}^h(x_1)\, f_i^{h'}(x_2)\right]$$

$$\frac{d^2\sigma}{dMdx} = \frac{8\pi\alpha^2}{3M^3}\frac{1}{3}\sum_i \frac{Q_i^2}{x_1 + x_2}\left[f_i^h(x_1)\, f_{\bar{i}}^{h'}(x_2) + f_{\bar{i}}^h(x_1)\, f_i^{h'}(x_2)\right].$$

In the present experiment we have been proceeding in two steps:

(a) Experimentally testing the DY model,

(b) Application of the pion structure function.

Concerning the first point there are a number of specific features of dimuon production which must be satisfied in the high mass continuum if the DY model is correct.

(a) A-dependence: incoherence of $\bar{q}q$ annihilation → cross section $\propto A$.

(b) Charge asymmetry:

$$\frac{\sigma(\pi^+ N)}{\sigma(\pi^- N)} \propto \frac{\bar{d}d}{\bar{u}u} \text{ (for large } \tau) \begin{matrix} \rightarrow 1/4\ I \\ \rightarrow 1/8\ H_2 \end{matrix} = 0 \text{ target (assuming } u = 2d).$$

(c) Decay angular distribution: $\gamma_V(1^-) \rightarrow 1 + \lambda\cos^2\theta \rightarrow \lambda = 1$.

(d) Scaling: $M^3 d\sigma/dM = f(M/\sqrt{s})$.

(e) Absolute cross section: predictable for reactions with known structure functions.

2.2.1 A-dependence of the DY cross section

Due to the incoherent nature of the quark annihilation process in the D.Y. model, the target acts like an assembly of free quarks, the cross section is therefore expected to be linear in $A^{(*)}$, i.e. $\sigma_{DY} \sim A^{\alpha}$ with $\alpha = 1$, contrary to purely hadronic reactions.

In our analysis we compare the H_2 with the Pt data (table 2). We take advantage of having both π^- and π^+ data: by using the cross section difference $\sigma = \sigma(\pi^-) - \sigma(\pi^+)$ we eliminate sea effects.

We measure

$$A \frac{\sigma(H)}{\sigma(Pt)} = 1.51 \pm 0.28$$

$$= A^{1-\alpha} R(x_2) \text{ where}$$

$$R(x_2) = \frac{4u - d}{u + 2d} = \frac{\sigma(\pi^- - \pi^+) \text{ on } H_2}{\sigma(\pi^- - \pi^+) \text{ on Pt}} .$$

We have used two relations u vs. d:

(a) $u = 2d \rightarrow R(x_2) = 7/4 = 1.75$ or

(b) $2d/u = 1.125(1 - x) \rightarrow R(x_2) = 1.8$ at $\langle x_2 \rangle^{\text{expt.}} = 0.15$

thus

$$A^{\alpha-1} = \frac{1.80}{1.51} \rightarrow \alpha_{DY} = \underline{1.03 \pm 0.03} .$$

Other experiments find:

$\alpha = 1.02 \pm 0.2$ for p on Be, Cu, Pt (CFS Collaboration, [9]).

$\alpha = 1.12 \pm 0.05$ for π^- on Cu, C, W (CIP Collaboration, [10]).

The latter may have to be reconsidered, however, since it also leads to non-scaling of the CIP data, as discussed below. CIP and NA3 agree as far as the per-nucleus cross section is concerned.

(*) Taking into account the isospin asymmetry of the nucleus.

2.2.2 Charge asymmetry

The electromagnetic nature of the DY process implies that differently charged quarks produce different annihilation cross sections. This leads to a charge-asymmetry in contrast to hadronic processes. Example:

$$\frac{\pi^+ p}{\pi^- p} = \frac{\bar{d}d}{2\,\bar{u}u} \to \frac{1/9}{2x4/9} = 1/8 \text{ on } H_2$$

$$\frac{\pi^+ \text{ nucleon}}{\pi^- \text{ nucleon}} \to 1/4 \text{ for a I = 0 target}$$

} in the limit of $M/\sqrt{s} \to 1$, i.e., in the approximation that the sea quarks are neglected and that the x distributions of u and d are the same.

The exact asymptotic value depends on the I spin composition of the target as well as on the structure functions.

The experimental data closely reproduce this most striking prediction of the DY model as shown in fig. 9.

2.2.3 Angular distribution

A $1 + \lambda\cos^2\theta$ distribution with $\lambda = 1$ (for instance in the Gottfried-Jackson frame) is expected because of the intermediate photon γ_v. The experimental data agree within errors, as seen in fig. 10.

Notice that in fig. 10 we have limited the transverse momentum to $Pt \lesssim 1$ GeV/c; this is because at large Pt and/or large x, the picture becomes more complicated since $\sin^2\theta$ terms are expected [10].

2.2.4 Scaling

Scaling in the form $M^3 d\sigma/dM = f(M/\sqrt{s})$ is an inherent feature of the DY process. Our data at 200 and 280 GeV/c (fig. 10) support this hypothesis, as well as the pN data of ref. [9] at higher energies. The data of the CIP Collaboration [10] are in apparent disagreement (factor ~ 2 below NA3, fig. 11); this is probably related to their extraction of the "per nucleon" cross section through non-linear $A^{1.12}$ dependence, as mentioned above.

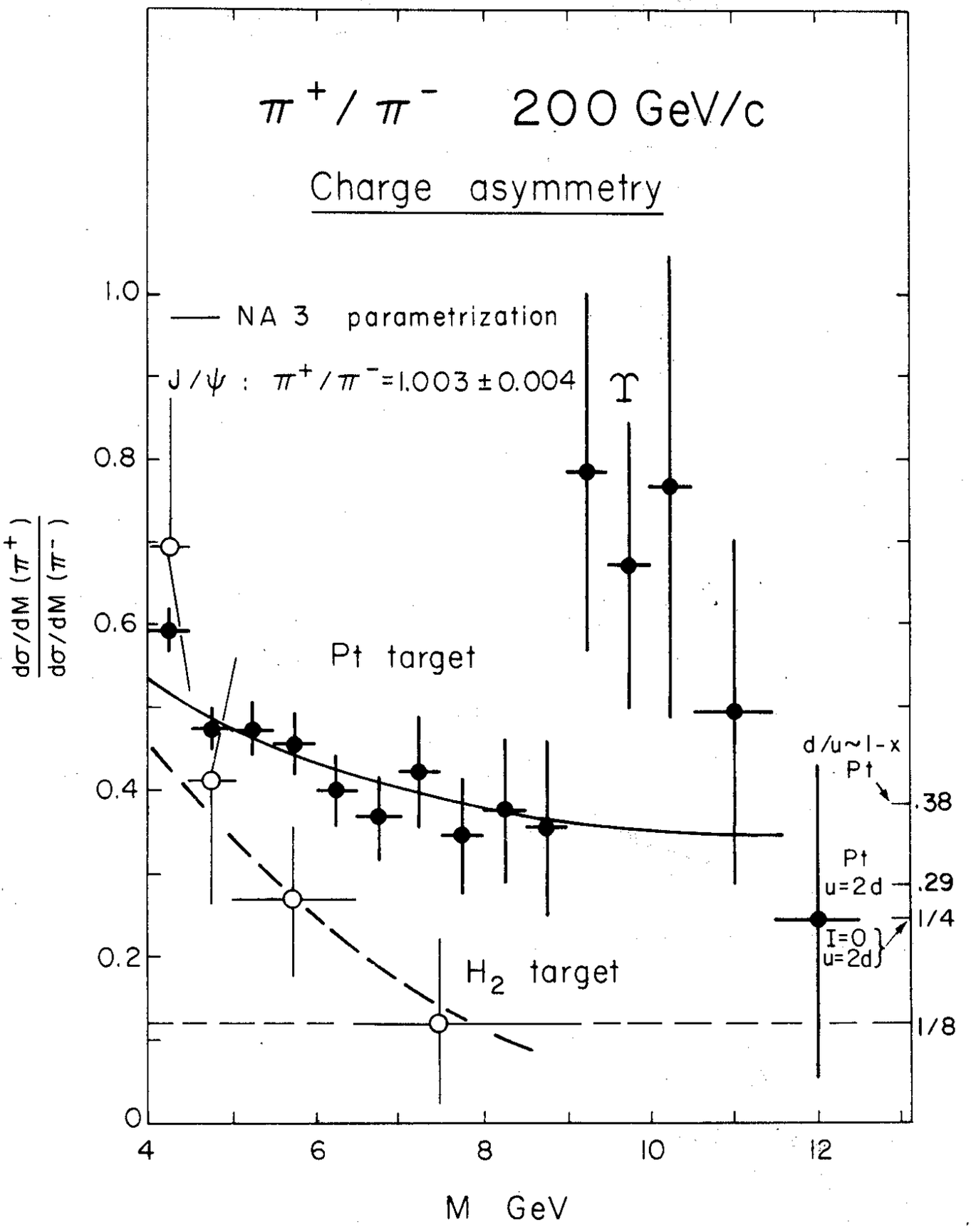

Fig. 9 Charge asymmetry of the D.Y. process

Decay angular distribution

$1 + \lambda \cos^2 \theta^*$

Gottfried - Jackson : $\lambda = 0.80 \pm 0.17$

Collins - Soper : $\lambda = 0.85 \pm 0.17$

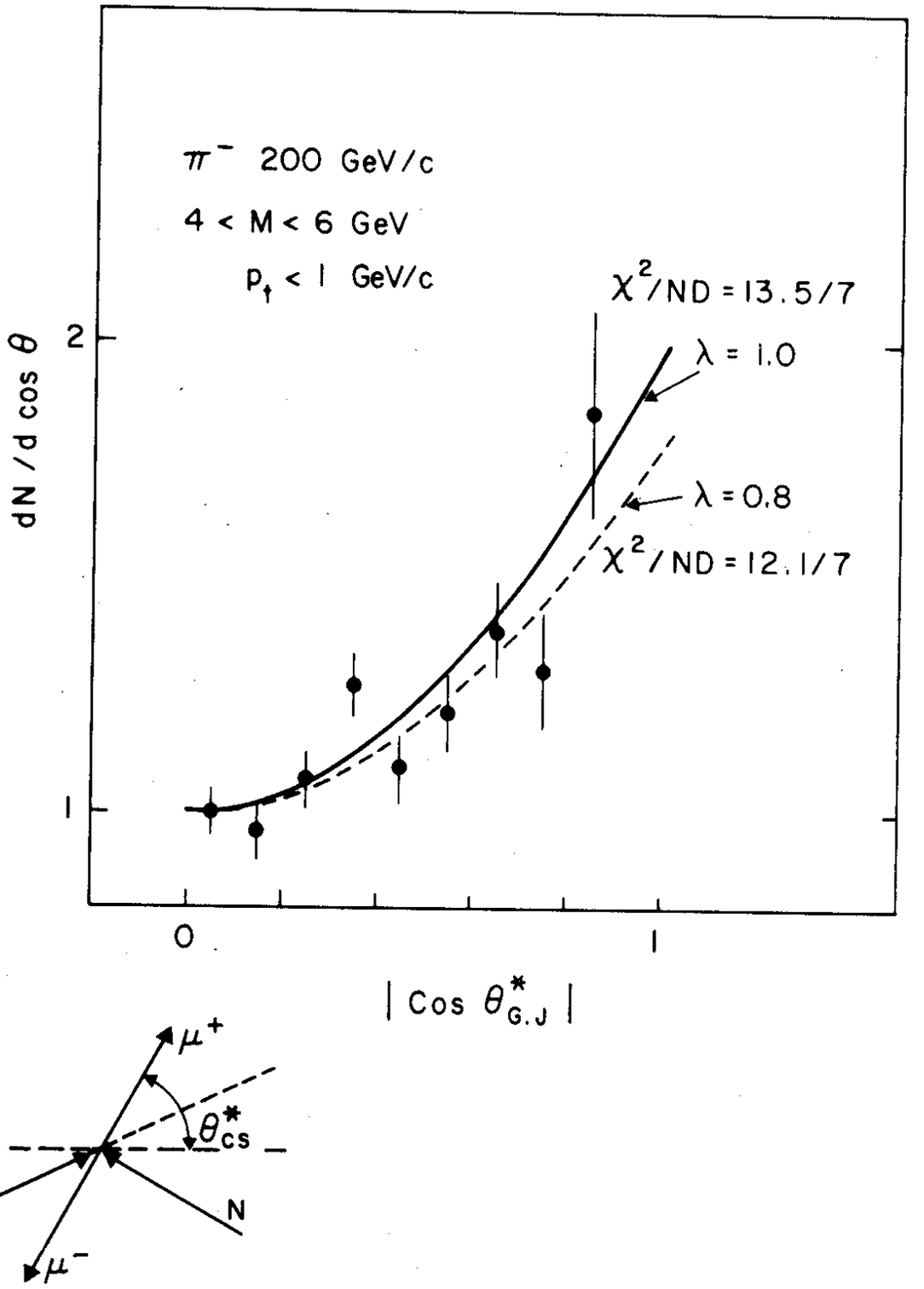

Fig. 10 Decay angular distribution.

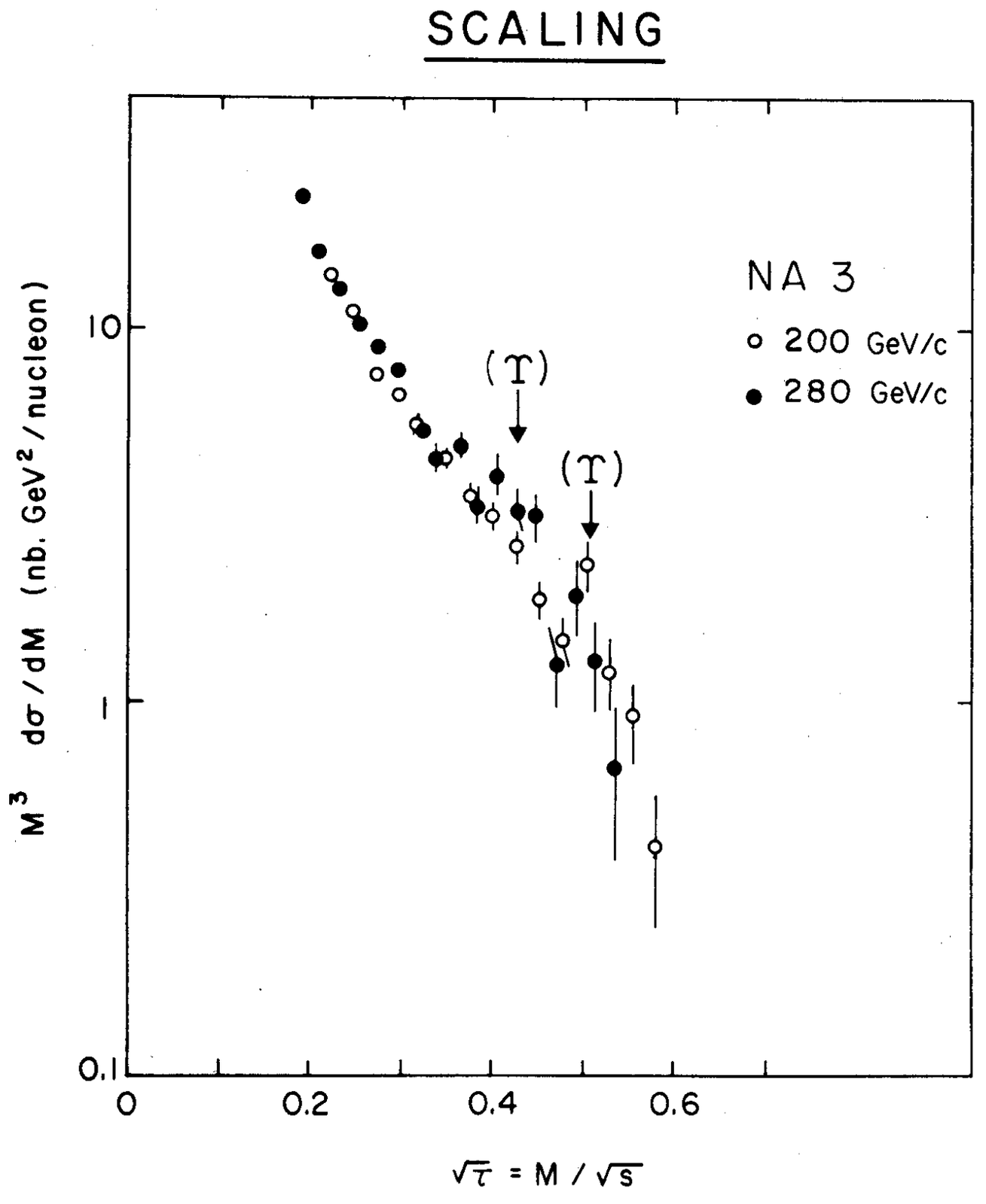

Fig. 11 Scaling of $M^3 d\sigma/dM$.

Notice that the log Q^2 dependence observed for instance in deep inelastic lepton scattering is too small to be detected in our data (5% effect in our range of Q^2).

2.2.5 Absolute value of the DY cross section

Tests (a)-(d) discussed above are well described by the DY process and one would conclude up to here that the model is essentially correct. There are, however, two experimental facts to complicate the situation.

(a) Large Pt events, i.e. about half of the di-muons have Pt $\gtrsim$ 1 GeV/c. There are two comments to make here, first, the DY model assumes $p_t = 0$ therefore whatever p_t distribution found experimentally cannot be regarded as a test of the model. Secondly, the fact that a substantial fraction of the events is above what one can reasonably assume as "primordial" p_t of the quarks (i.e. their "Fermi motion" in the nucleon, for instance 0.3 - 0.7 GeV/c) goes beyond the simple quark model; additional mechanisms are needed.

(b) The absolute cross section of the DY process in determined as

$$\frac{d^2\sigma}{dx_1 dx_2} = \frac{4\pi\alpha^2}{3s} \cdot \frac{1}{3} \cdot \sum_i \frac{Q^2 i}{x_1{}^2 x_2{}^2} \left\{ f_i(x_1)\ \bar{f}_i(x_2) + \bar{f}_i(x_1)\ f_i(x_2) \right\} , \quad (1)$$

where the Q_i are the quarks fractional charges and $f_i(x_1)$, $f_i(x_2)$ are the effective structure functions of the projectile and target particles respectively. The so-called "naive" model does therefore not contain any free parameter and the absolute value of the cross section is predicted exactly for reactions where both the projectile and target particle (i.e. their structure function) are known, for instance for $p(\bar{p})N$ known from deep inelastic lepton scattering experiments.

The present experimental data allow us to check this prediction in quantitative detail. For the first time, deviations from the simple DY model have been found.

If we express the ratio of measured over the expected DY cross section by a scale factor K defined as

$$\sigma(DY)_{exp.} = K\sigma(DY)_{theory}$$

we find that $K \approx 2.3$ from five independent reaction channels at 200 GeV/c pN, $\bar{p}N$, $\pi^{\pm}N$ (for Pt), and $\pi^{-}H_2$.

The values of the K factor in the different channels are summarised in table 4.

TABLE 4

Summary $\sigma_{DY}^{exp.}/\sigma_{DY}^{theor.} = K$

Reaction	pN	$\bar{p}N$	$\pi^{-}N$	$\pi^{+}N$	$\pi^{-}H_2$	$\pi^{-}-\pi^{+}$
K	2.2 ± 0.3	2.4 ± 0.5	2.2 ± 0.3	2.4 ± 0.4	2.4 ± 0.4	2.2 ± 0.4

2.4 ± 0.5

$\langle K \rangle = 2.3$ (± 0.5 systematic error).

The following specific remarks should be made:

2.2.5.1 pN data

(a) The nucleon structure function from DY

The practical use of the DY mechanism to measure structure functions of unstable hadrons can be tested directly by comparing the proton structure function obtained from DY data with that from deep inelastic lepton scattering (at equal $Q^2 = -M^2$ (*)). NA3 is in a good position to perform such a study because of its large acceptance. This comparison is essential in order to justify the use of structure functions from deep inelastic lepton scattering to predict the "theoretical" DY cross section.

Our pN data were obtained at 200 GeV/c with a mixed positive beam (table 1) incident on a 6 cm platinum target. There are 1300 proton induced dimuon events in the mass region above 4 GeV useful for a DY type analysis; their mass distribution is shown in fig. 12.

(*) We assume in this analysis that the Buras-Gaemers parametrization of the structure functions is applicable equally in the spacelike (DIS $Q^2 < 0$) and timelike (DY $Q^2 > 0$) region.

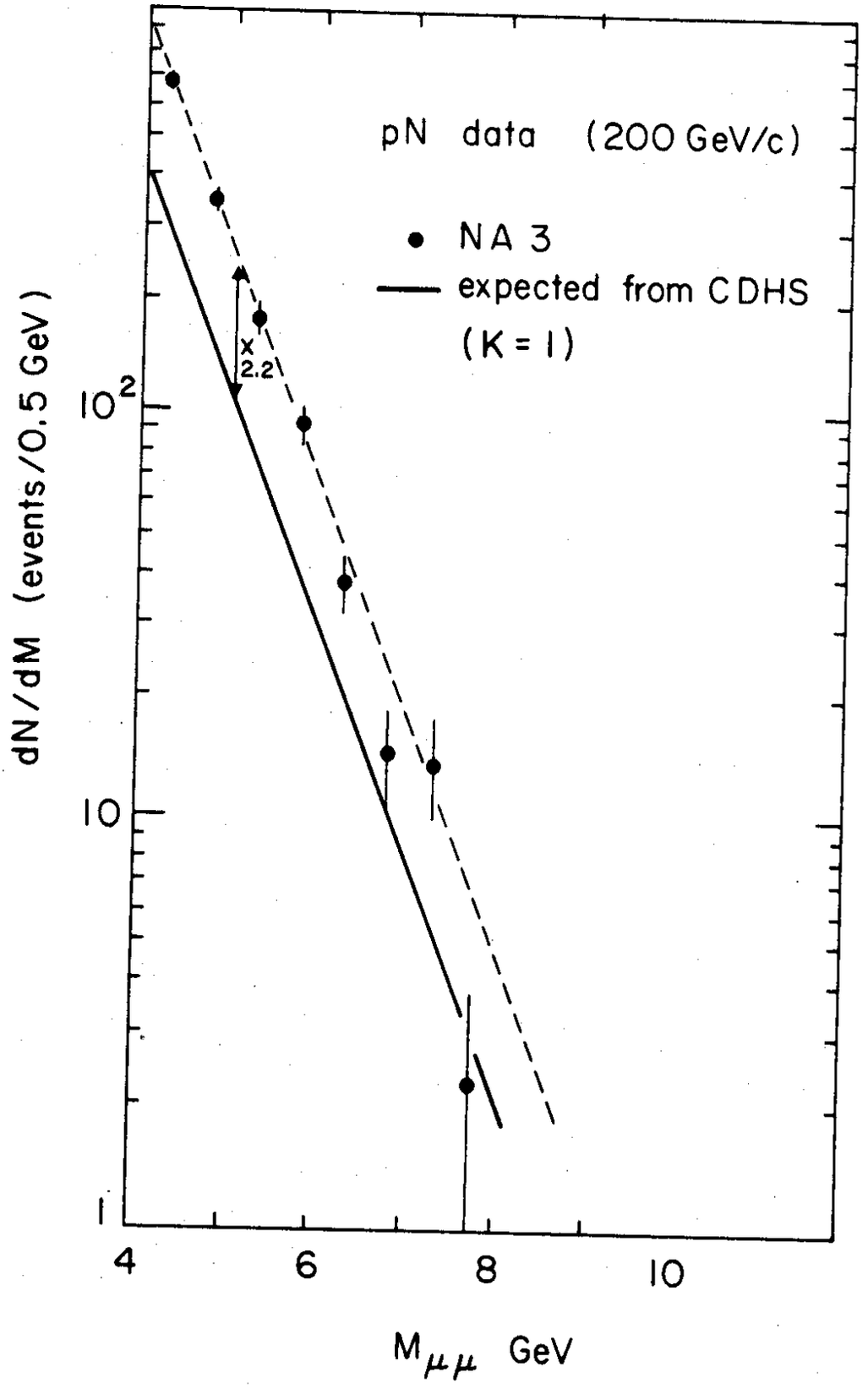

Fig. 12 Mass spectrum for pN events at 200 GeV/c; compared to prediction from CDHS nucleon structure function.

The data have been analysed as follows:

(i) Parametrization of the proton

$$\text{valence} \begin{cases} u^p = A_{\alpha\beta}^{\ u}\, x^{\alpha}(1-x)^{\beta} & \text{with } \int \frac{u^p}{x}\,dx = 2 \\ d^p = A_{\alpha\beta}^{\ d}\, x^{\alpha}(1-x)^{\beta+1} & \text{with } \int \frac{d^p}{x}\,dx = 1 \end{cases}$$

$$\text{sea} \begin{cases} \bar{u} = \bar{d} = A_s(1-x)^{\beta_s} \\ \bar{s} = 1/4(\bar{u} + \bar{d}) \leftarrow \text{CDHS result [11]} \end{cases}$$

α, β, β_s free parameters

$\langle G \rangle$: average fractional momentum carried by gluons: fixed

A_s determined by $5A_s/(\beta_s + 1) = 1 - \langle G \rangle - \langle u \rangle - \langle d \rangle$.

(ii) Results of the fit

The parameters of the proton structure function from the DY data are compared to the DIS data (CDHS) in table 5.

TABLE 5

Parameters of the proton structure

	NA3	CDHS ($Q^2 = 20$)
$\langle G \rangle$	0.5 (fixed)	0.5
α_u	0.5 ± 0.2	0.51 ± 0.02
β_u	3.2 ± 0.4	2.8 ± 0.1
$\langle u + d \rangle$	32%	34%
β_s	9.4 ± 1.0	8.1 ± 0.7
A_s	0.37	0.27
$\langle sea \rangle$	18%	15%

Fig. 13 shows the agreement between our data and the CDHS nucleon parametrization.

Conclusion: - first determination of the nucleon valence structure using μ pairs,
- good agreement between DY and DIS determination of the nucleon structure.

(b) The absolute cross section

Since our analysis has shown that the DY nucleon structure parameters agree in shape with CDHS at equal $|Q^2|$, we can now use the latter as input to compute the DY cross section and derive K by comparison with the experiment; this leads to the $K = 2.2 \pm 0.3$ (table 4).

2.2.5.2 $p\bar{N}$ data

The weak point in determining K from pN data is the necessity of fixing the percentage of sea-quarks to the value found in the lepton scattering experiments (e.g. CDHS data), since one cannot, in principle distinguish in a DY experiment between, say $K = 2$ and a twice larger sea.

The cleanest experimental way of obtaining K is using antiprotons since in $\bar{p}N$ reactions the valence-sea terms contribute only < 15% to the DY cross section.

The $\bar{p}$ experiment is however difficult and we have collected so far only 44 DY events with $M > 4$ GeV, at 200 GeV/c on Pt; they are shown in fig. 14.

We obtain $K(\bar{p}N) = 2.4 \pm 0.5$.

This result would mean that the result K(pN) (last paragraph) cannot be due to an increased percentage of sea in the DY reaction, as compared to lepton scattering.

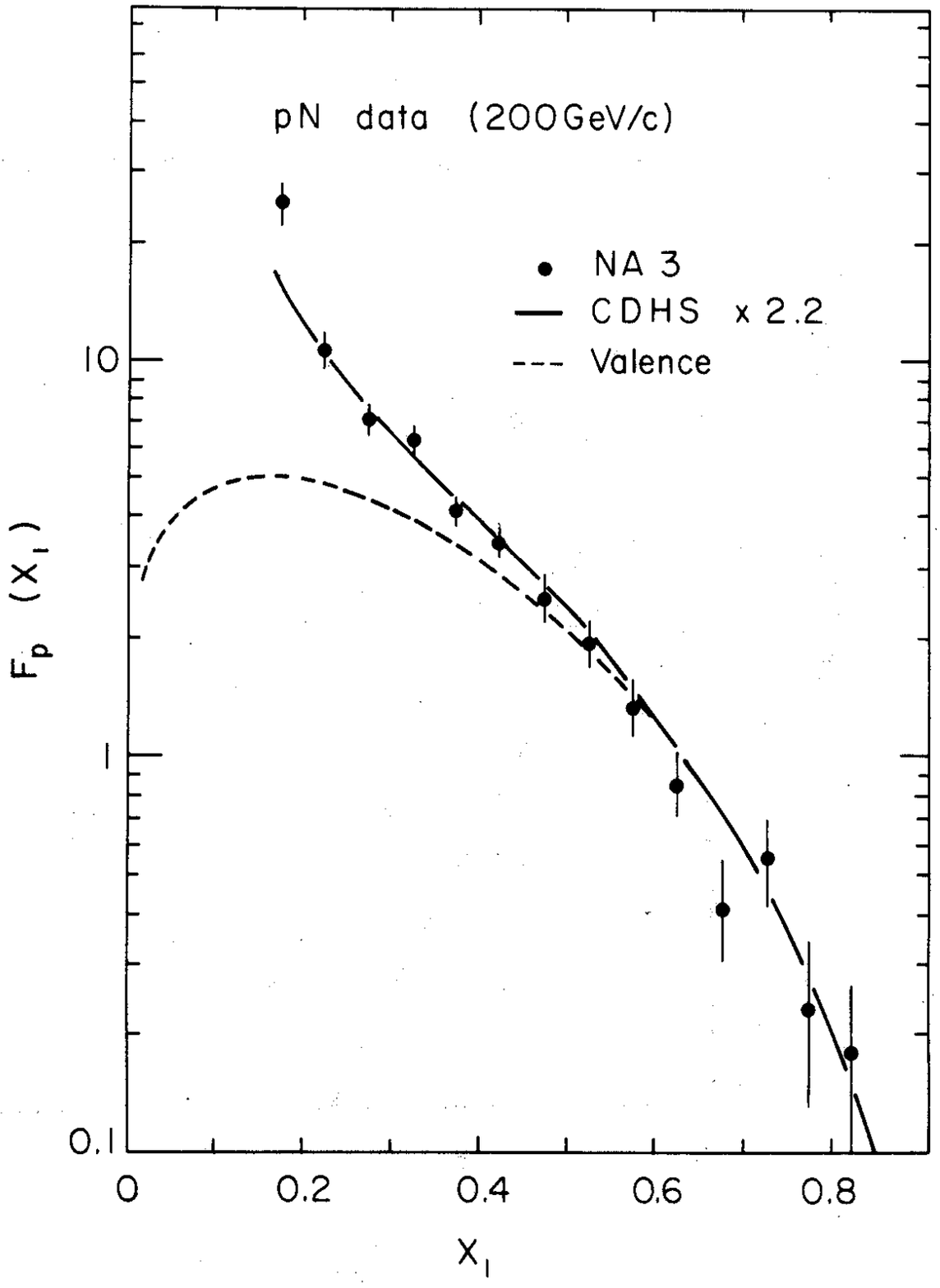

Fig. 13 NA3 proton structure function vs. CDHS at $Q^2 = 20(GeV/c)^2$.

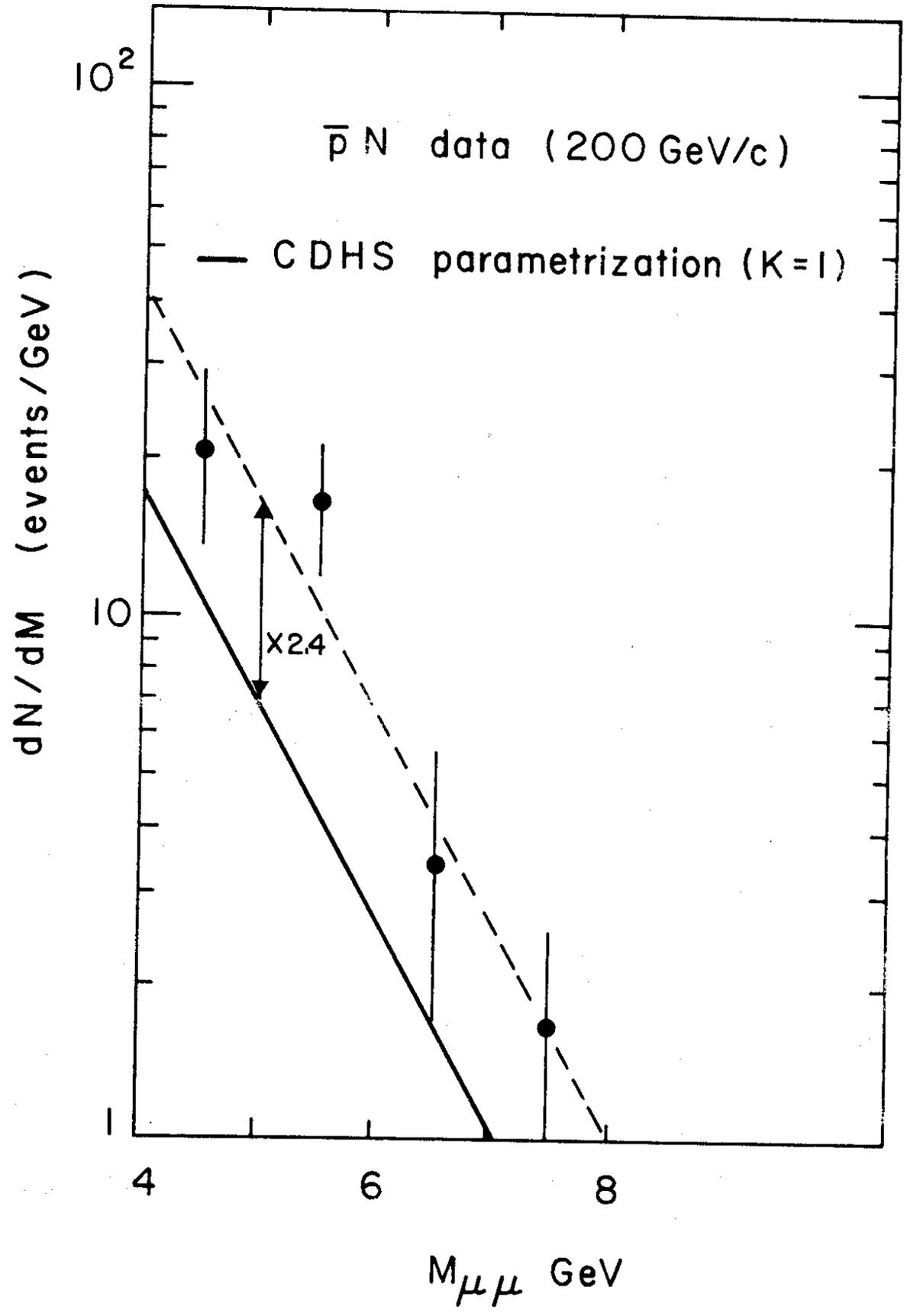

Fig. 14 $\bar{p}$ induced di-muon mass spectra vs. expectation from CDHS data.

2.2.5.3 π data

Pion data are in principle similar to $\bar{p}$ as to the dominance of the valence-valence term; however the definition of K is less direct since the π structure function cannot be determined independently by lepton scattering. On the other hand our analysis in ref. [4] shows that the π structure function is insensitive to details of the target nucleon since x_1 and x_2 are almost uncorrelated; we use

$$F_\pi^{val}(x_1) \sim x_1^{0.4} (1 - x_1)^{0.9} \text{ (for details see sect. 2.3).}$$

(a) $\pi^{\pm}$ - Pt data

We refer to ref. [4] for a detailed description of the method of analysis. The data are shown in fig. 15 for π^+ and π^-, giving $K = 2.4 \pm 0.4$ and 2.2 ± 0.3 respectively.

We have also analyzed the $\pi^- - \pi^+$ difference which has the advantage that sea effects and possible contributions from hadronic sources of dimuons are eliminated; this analysis leads to $K = 2.2 \pm 0.4$.

(b) $\pi^- - H_2$ data

A more direct way of measuring K with π^s is to use a H_2 target. This has the advantage that A = 1 and therefore no A-dependence is involved. From our 138 $\pi^- H^2$ events with $M > 4$ GeV we obtained $K = 2.4 \pm 0.4$. The data are shown in fig. 16.

We also note that the CIP Collaboration found $K \approx 1$ for $\pi^- W$ at 225 GeV/c [10]; this result is probably related to their $A^\alpha = A^{1.12}$ which leads to a factor of 2 in the "per-nucleon" cross section for A = 195 of the experiment and is compatible with $K \approx 2$.

The Goliath Collaboration $\pi^- Be$ at 150 GeV/c [12] finds $K \approx 3$ assuming again a linear A dependence.

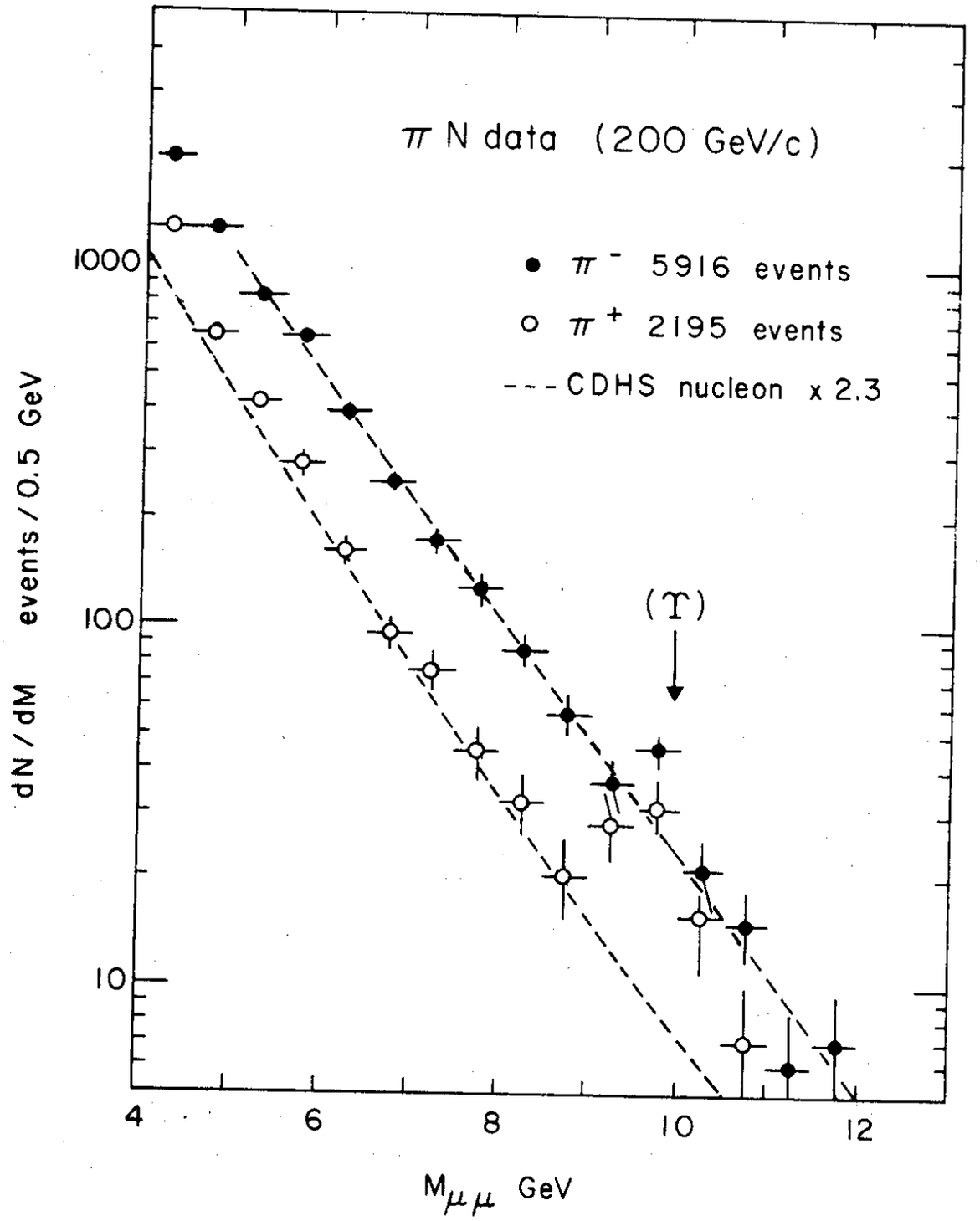

Fig. 15 $\pi^{\pm}$ induced di-muon mass spectrum compared to expectation using CDHS nucleon structure.

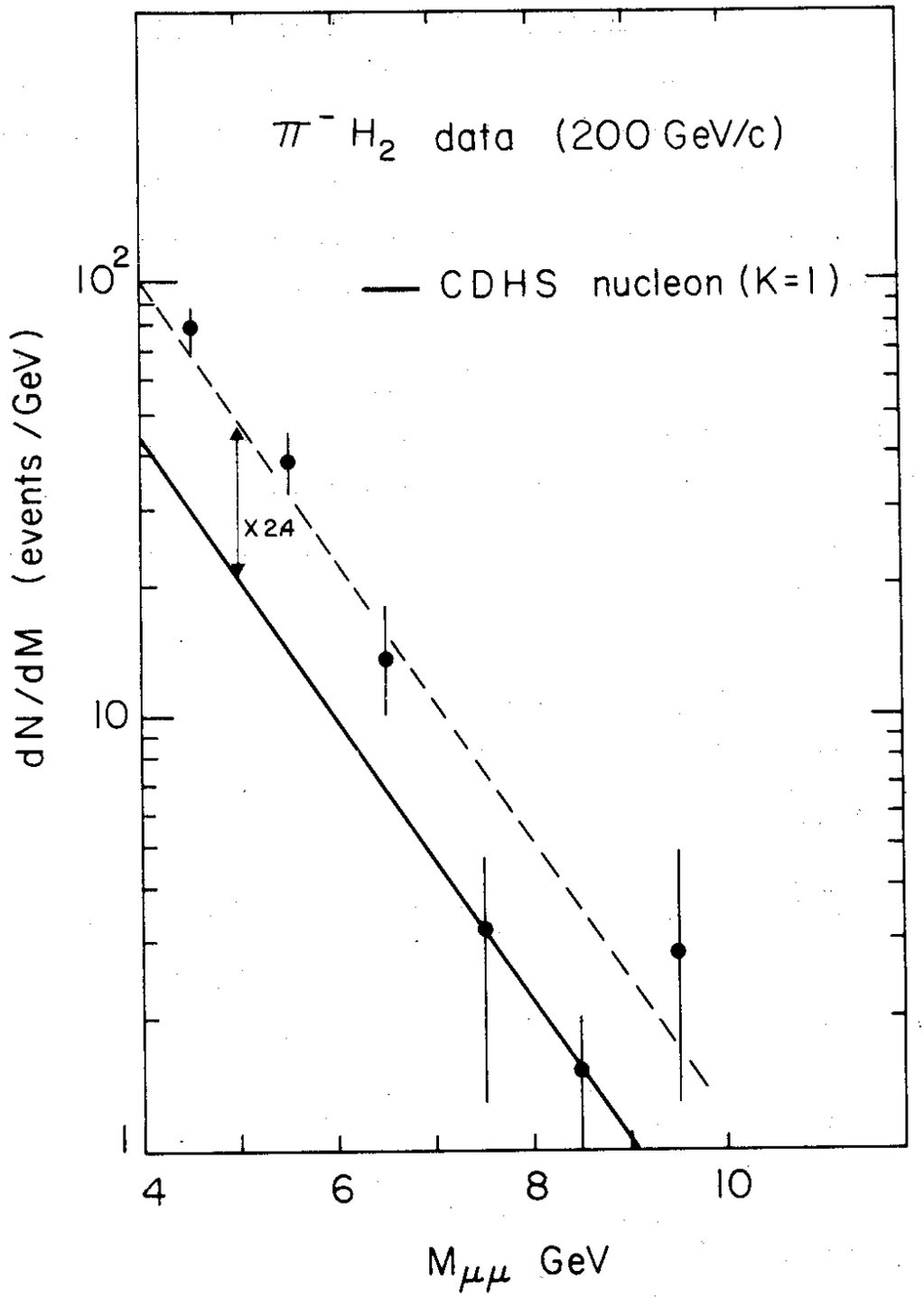

Fig. 16 Di-muon mass spectrum for $\pi^- H_2$ data.

2.2.5.4 Conclusions concerning the absolute DY cross section

In conclusion the absolute experimental DY cross section is larger than expected from the so-called "naive" DY model (using deep inelastic nucleon structure functions as input) by a factor of about two.

An effect of this size has been predicted by theory due to first order QCD corrections to the normal DY formula (for a review see [13](*)).

Di-muon production by antiprotons may be a good test of QCD corrections to the DY model. NA3 is now concentrating on this channel with the aim of gaining about an order of magnitude on our present data.

A more detailed discussion of the K factor in the different reaction channels will be published elsewhere [14].

2.3 Structure function of the pion

Pion-nucleon data at 200 GeV/c (fig. 17).

(a) Definitions

$$\frac{d^2\sigma}{dx_1 dx_2} = \frac{4\pi\alpha^2}{3s}\frac{1}{3}\frac{1}{x_1^2 x_2^2}\left[V_\pi(x_1)\,G(x_2) + S_\pi(x_1)\,H(x_2)\right]$$

(beam: V_π, S_π; target: G, H)

(i) Valence

π: $v_\pi(x_1) \equiv u_v^{\pi^-} = d_v^{\pi^-} = u_v^{\pi^+} = \bar{d}_v^{\pi^+}$

Nucleon: $\begin{cases} u(x_2) \equiv u_v^p = d_v^n \\ d(x_2) \equiv d_v^p = u_v^n \end{cases}$

Sea: $S_\pi(x_1)$, $S_n(x_2)$

(*) However, the apparent numerical agreement may be fortuitous since higher order corrections in α_s have not been calculated yet and can be large, too.

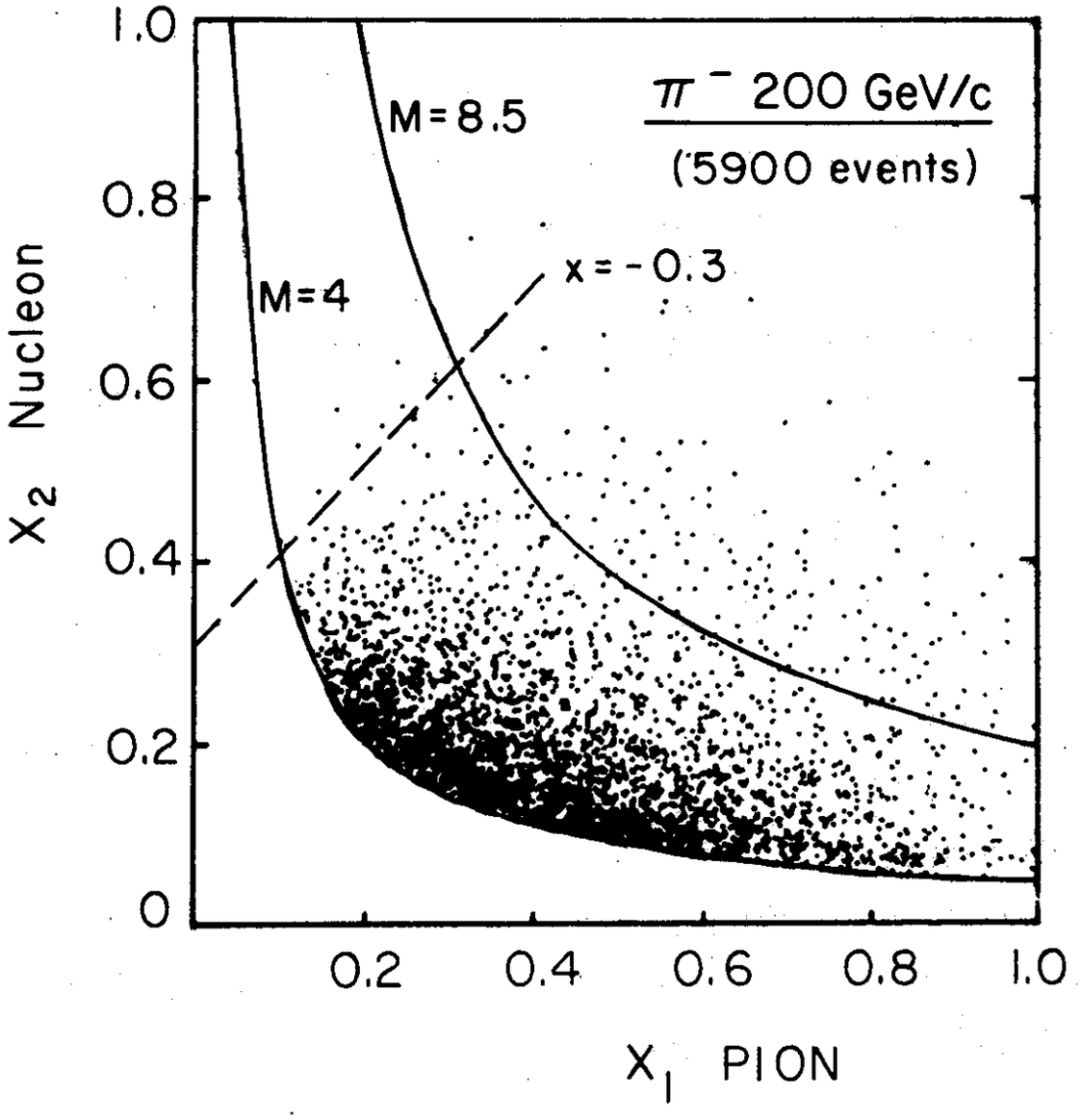

Fig. 17 x_1 - x_2 scatter plot for π^- events at 200 GeV/c.

(ii) Normalisation of quark number

$$\int \frac{v_\pi(x_1)}{x_1}\,dx_1 = 1, \quad \int \frac{u(x_2)}{x_2}\,dx_2 = 2, \quad \int \frac{d(x_2)}{x_2}\,dx_2 = 1.$$

Pt target ($I \neq 0$) : $Z/A = 0.4$

$G(x_2) = 1/9\ (1.6u + 2.4d + 5S_n)$ for π^-

$G(x_2) = 1/9\ (0.6u + 0.4d + 5S_n)$ for π^+

$H(x_2) = 1/9\ (2.2u + 2.8d + 12S_n)$ for π^+, π^-

(b) Parametrization of the π, N structure functions

Nucleon	Pion
$u(x_2) = A_u x_2^{\alpha_u}(1 - x_2)^{\beta_u}$	$V_\pi(x_1) = A_\pi x_1^{\alpha_\pi}(1 - x_1)^{\beta_\pi}$
$d(x_2) = A_d x_2^{\alpha_u}(1 - x_2)^{\beta_u + 1}$	$S_\pi(x_1) = B_\pi(1 - x_1)^{\beta_\pi^s}$
$S(x_2)$: $\bar{u} = \bar{d} = A_s(1 - x_2)^{\beta_u^s} = \bar{s}$	

(c) Results

Nucleon		Pion	
CDHS = input ($Q^2 = 20$) [11]			
$\alpha_n = 0.51 \pm 0.02$	mom. fractions	$\alpha_\pi = 0.37 \pm 0.02$	mom. fractions
$\beta_n = 2.8 \pm 0.1$	val. = 34%	$\beta_\pi = 0.92 \pm 0.03$	val. = 32%
$\beta_n^s = 8.1 \pm 0.1$	sea = 15%	$\beta_\pi^s = 5$ fixed	sea = 13%

(d) Conclusion

$$F_\pi^{val.} \sim x^{0.4 \pm 0.1}(1 - x)^{0.9 \pm 0.1}$$ (fig. 18).

This result is independent of details of the target structure function.

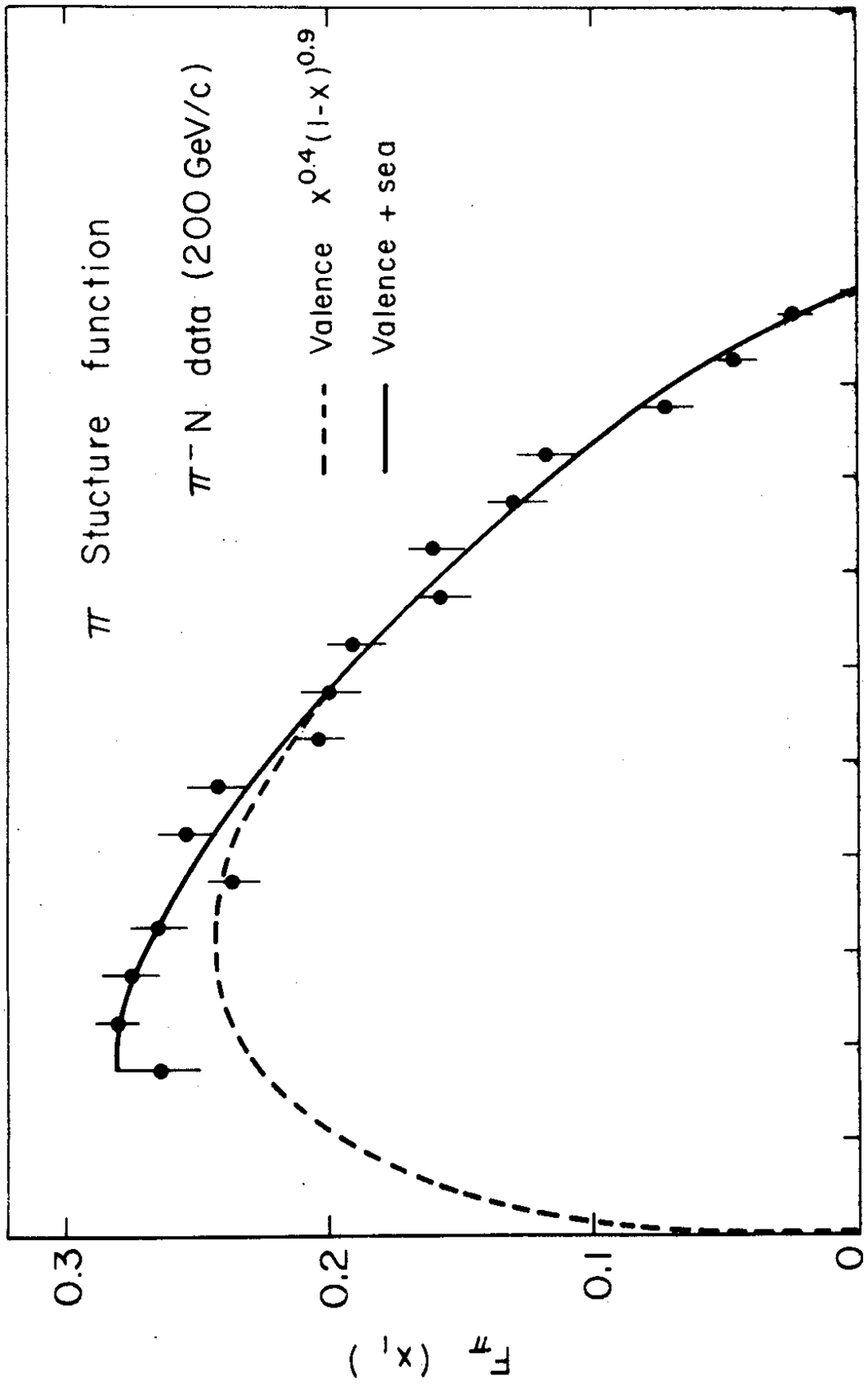

Fig. 18 The π structure function.

3. SUMMARY AND CONCLUSIONS

(a) Upsilon: first evidence for T production by pions

$$\sigma(\pi) \gtrsim 30\ \sigma(p) \quad \text{and} \quad B\sigma(T)/B\sigma(\psi) \approx 2 \times 10^{-4} \ .$$

(b) Muon pair continuum:

"Drell-Yan mechanism":
- A-dependence
- charge asymmetry
- angular distribution
- scaling

} classical Drell-Yan model works

But: absolute experimental cross section > Drell-Yan model predictions by factor K = 2.3 (± 0.5).

(c) Pion structure function:

$$F_\pi^{val.} \sim x^{0.4 \pm 0.1} (1-x)^{0.9 \pm 0.1}$$

REFERENCES

[1] J. Badier et al., First evidence for upsilon production by pions, Phys. Lett. 86B (1979) 98.

[2] J. Badier et al., Di-muon resonance production from 200 and 280 GeV/c tagged hadron beams, Int. High Energy Physics Conf., Geneva 1979.

[3] J. Badier et al., Muon pair production at masses above 4 GeV (Drell-Yan Continuum), Int. High Energy Physics Conf., Geneva 1979.

[4] J. Badier et al., Experimental determination of the pion and nucleon structure functions by measuring high mass muon pairs, Int. High Energy Physics Conf., Geneva, 1979.

[5] J.K. Yoh et al., Phys. Rev. Lett. 41 (1978) 684.

[6] I. Mannelli, Electron pair production at the ISR, Proc. 19th Int. Conf. on High Energy Physics (Tokyo 1978), Physical Society of Japan, Tokyo (1979) 189.

[7] A.L.S. Angelis et al., A measurement of the production of massive e^+e^- pairs in p-p collision at $\sqrt{s}$ = 63 GeV, presented at the EPS Int. Conf. on High Energy Physics, Geneva, 1979.

[8] D. Antreasyan et al., Dimuon spectra from 62 GeV proton collisions, presented at the EPS Int. Conf. on High Energy Physics, Geneva 1979.

[9] L.M. Lederman, Dilepton production in hadron collision, Proceedings of the 19th Int. Conf. on High Energy Physics, Tokyo 1978, and closing remarks, this Conference.

[10] J. Pilcher, Review of di-muon production in Hadron collision, this Conference.

[11] For a review of the results of the CDHS Collaboration see for instance: A. Para, Recent measurements of nucleon structure functions from neutrino scattering, this Conference.

[12] R. Barate et al., Production of high-mass muon pairs in π^- Be collision at 150 and 175 GeV/c, submitted to Phys. Rev. Lett. and CERN/EP 79-87.

[13] G. Altarelli, Lepton pair production, presented at the EPS Int. Conf. on High Energy Physics, Geneva, 1979.

[14] J. Badier et al., Cross section of dimuon production in hadron collision and the Drell-Yan model, to be submitted to Phys. Letters.